Airborne lidar measurements of atmospheric pressure made using the oxygen A-band

Haris Riris[1], Michael D. Rodriguez[2], Graham R. Allan[2], William E. Hasselbrack[2], Mark A. Stephen[1], James B. Abshire[1],

[1]NASA GSFC, Greenbelt, MD 20771, USA
[2]Sigma Space Corp, 4400 Lottsford Vista Road, Lanham, Maryland 20706, USA

ABSTRACT

We report on the atmospheric pressure measurements using a fiber-based laser system using the oxygen A-band at 765 nm. Remote measurements of atmospheric temperature and pressure are required for a number of scientific applications including greenhouse gas monitoring, weather prediction, and climate modeling.

Keywords: Oxygen Measurements, Lidar, ASCENDS, Space Instrumentation

1. INTRODUCTION

Accurate measurements of greenhouse gas mixing ratios on a global scale are currently needed to gain a better understanding of climate change and its possible impact on our planet. The most important greenhouse gas of interest is presently carbon dioxide but other gases such as methane and carbon monoxide are also significant contributors to climate change. The ultimate goal of CO_2 remote sensing is to derive CO2 concentrations in the atmosphere in terms of mole fraction in unit of parts-per-million (ppmv) with regard to dry air. Therefore, both CO2 and dry air number of molecules in the atmosphere are needed in deriving this quantity. O2 is stable and uniformly mixed in the atmosphere. The measurement of O2 absorption in the atmosphere can thus be used to infer dry air number of molecules and then be used to calculate CO2 concentration. With the knowledge of atmospheric water vapor, we can further estimate the total surface pressure that can be used to better define both O2 and CO2 line shapes for better retrievals, as both CO2 and O2 absorptions in the near infrared are a function of pressure as well as temperature.

Oxygen is stable and uniformly mixed in the atmosphere. Its dry mixing ratio stays constant at 20.95%. This measurement concept has been previously demonstrated earlier [1–4] but was hampered by limitations in the laser and detector technology. Our technique of measuring pressure uses several on- and off-line wavelengths tuned to an O_2 absorption line in the A-band at 764.7 nm (Figure 1). The choice of wavelengths allows us to maximize the pressure sensitivity using the trough between two absorptions in the Oxygen A-band. Our retrieval algorithm fits the O_2 lineshapes and derives the pressure from the profiles of the two lines. The O2 lines were selected after careful spectroscopic analysis to minimize the temperature dependence and analysis of the component technology to optimize the transmitter power, doubling efficiency, and detector sensitivity [5]. We have demonstrated O2 measurements from the ground and from an airborne platform. Our measurements compare favorably with a local weather monitor mounted outside our laboratory and a local weather station.
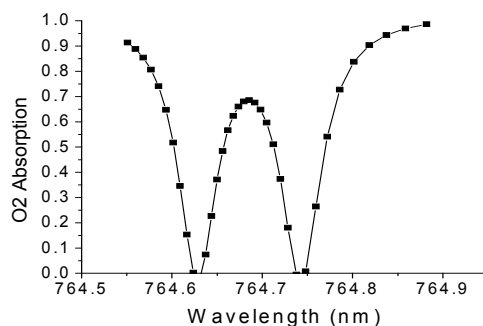

Figure 1 Oxygen absorptions used to measure pressure

2. INSTRUMENT DESCRIPTION

The present instrument uses a continuous wave (CW) distributed feedback (DFB) diode laser operating at 1529 nm (Figure 2). Its current and temperature are controlled by a commercial laser driver and the wavelength is adjusted to coincide with the O2 doublet absorption at 764.7 nm. The wavelength of the diode laser is rapidly tuned (250 Hz) over the O2 absorptions by applying a voltage ramp waveform to the drive current. The frequency and amplitude of the wavelength scan ramp waveform are easily adjusted using the computer-controlled waveform generator. A calibration procedure using heterodyne techniques, an external wavemeter and a stabilized 1529 nm laser source provides an accurate precise calibration of our wavelength scan. The instantaneous diode laser linewidth is very narrow (<10 MHz depending on the laser driver being used).

The output of the diode laser is then externally modulated (chopped) with a fiber-coupled acousto-optic modulator (AOM) to yield relatively short (100-500) ns laser pulses with a 30-40 dB extinction ratio. The number of pulses and the pulse width are easily adjustable by adjusting the pulse train waveform applied to the AOM. Typically, 40 pulses are used to trace the absorption lines but as few as 20 have been used in our experiments. The pulses are separated by 100 µs. The 100 µs time separation ensures that each wavelength pulse is received before the next one even in the presence of high altitude clouds that may scatter a pulse back into the receiver before it hits the ground. The last three pules of the 40 pulse train occur near or at the end of the ramp waveform and are not used in the analysis.

The pulses from the AOM are directed to an Erbium Doped Fiber Amplifier (EDFA) which amplifies them. The EDFA output is fiber-coupled into a periodically poled (PPLN) KTP crystal assembly which frequency doubles the 1529 nm radiation to 764.5 nm. The free-space output from the doubling crystal is directed to the transmit optics which include a beam expander to reduce the beam divergence to about 110 µrad and an integrating sphere with an energy monitor. The output of the energy monitor is integrated and then digitized by an analog to digital converter (A/D) to provide an accurate measure of the outgoing laser pulse energy.

For ground testing the beam is usually directed to a cooperative target placed on a cellular phone tower approximately 1.5 km away. For the airborne tests the transmitter light pulses travel through the nadir port of the airplane and onto the ground. The reflected light is collected by a commercial 20 cm diameter receiver telescope and is coupled into a large area (400 µm) multi-mode fiber. The field of view (FOV) of the receiver is determined by the effective focal length of the telescope (2 m) and the receiver fiber size. In our case the FOV is 200 µrad. The fiber output is collimated and goes through a narrow (0.5 nm) bandpass filter, an adjustable iris and onto a single photon counting module (SPCM). The output from the SPCM is amplified and then directed through a discriminator circuit with adjustable threshold. The output of the discriminator is sent to a multi-channel scaler which produces a histogram of the return pulses as a function of time (range).   The computer then digitizes and averages the returns over a 1 second interval. The averaging interval is also adjustable. For ground testing, where the return is very strong, the SPCM can be substituted with a silicon photodiode and the resulting waveforms are digitized and averaged by a fast analog to digital converter (A/D) instead of going to the discriminator and multi-channel scaler. The computer then digitizes and averages the returns over a 1 second interval. For ground testing a commercial weather station placed at the roof of our building serves as the "truth" for our pressure measurements.
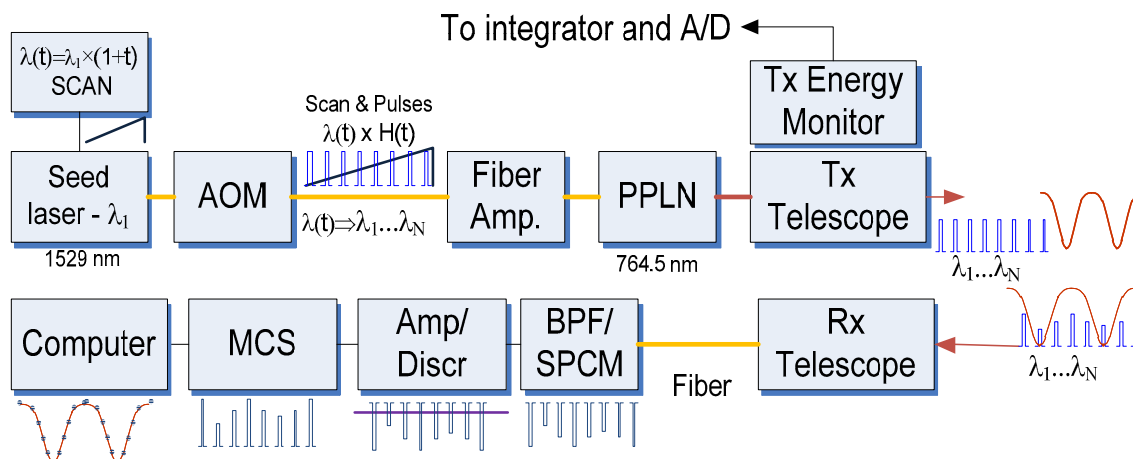

Figure 2 Experimental setup

3. EXPERIMENTAL RESULTS

1.1 Ground Testing

Over the course of several months in the summer and fall of 2009 we collected data (weather permitting) using our system and compared them with the weather station. A condensed version of the data is shown in Figure 3. The pressure is estimated by applying a Voigt fitting algorithm that minimizes the error between the theoretical lineshape, as calculated from the HITRAN 2008 database [6], and the experimental lineshape.
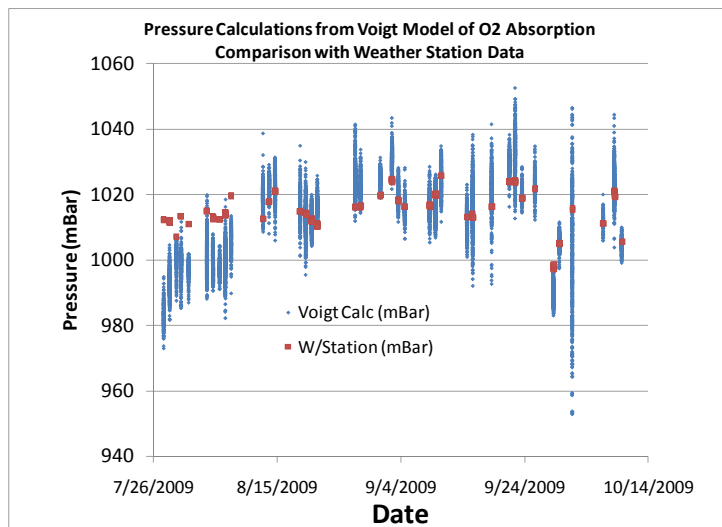

Figure 3 Pressure measurement comparison over 4 months between our O2 system (blue) and the weather station (red).

The data between the two instruments compare favorably over several months even though the O2 system seems to be noisier as a result of lower averaging compared to the weather station. There is also an occasional systematic offset between the two systems that varies over time. We have traced part of this offset to the energy monitor operation and the way we normalize the return pulses. We hope to improve our normalization and minimize the offset in the future. In the short term (~2 hours) the two systems agree very well (Figure 4) even though the O2 system is noisier for the reasons outlined above and there is a systematic offset. We will improve the averaging and reduce the random noise in the system by changing the data acquisition hardware and the way we perform the averaging.
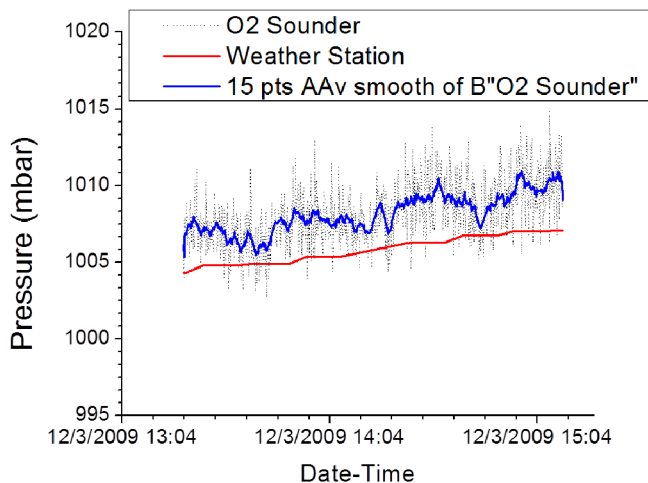

Figure 4 Short term (2 hour) comparison between our O2 system (blue) and the weather station (red).

1.23.2 Airborne Testing

In 2010 we participated in a joined airborne campaign sponsored by the NASA ASCENDS program to measure CO_2 and O_2 fluxes in the Western United States. The O_2 system was part of the GSFC CO_2 Laser Sounder [7]. A concept of the airborne operation is shown in Figure 5. Two beams one for CO_2 and one for O_2 exit the nadir port of the plane at slightly different angles (~ 500 µrad). Each beam has a divergence of 100-110 µrad which means at an altitude of 10 km the spot on the ground is approximately 1 m. For the O_2 system, a series of forty, 250 ns, pulses, each at a slightly different wavelength exit the aircraft, separated by 100 µs. At cruising speeds of 250 mph the separation between successive wavelength pulses on the ground is only 1 cm, thus minimizing any changes in the return pulse amplitude due to ground reflectivity. The returns are collected by a fiber coupled receiver which has two fields of view (FOV) one for CO_2 and one for O_2. The returns for O_2 are detected by the SPCM and processed by the amplifier/discriminator and MCS system described in section 2 above.
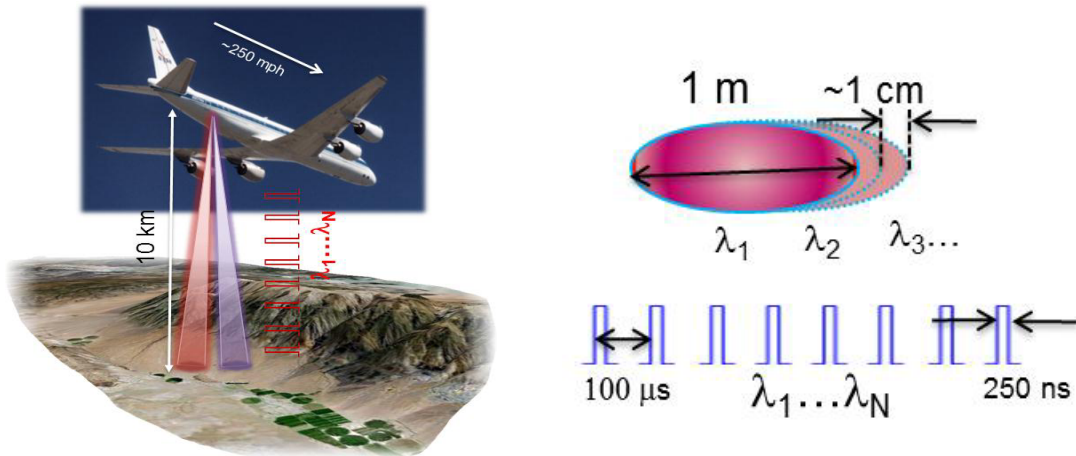

Figure 5 Airborne operations concept and pulse train and spots on the gournd

One of our 2010 flights was over the Pacific Ocean off the coast of the Baja peninsula. Figure 6 shows the flight path and altitude profile. The airplane provides ancillary data such as GPS position, altitude, pressure, temperature, humidity, etc. Using the pressure, temperature and humidity data and the HITRAN 2008 database we performed the radiative transfer calculations an derived the expected linsehapes at different flight altitudes.
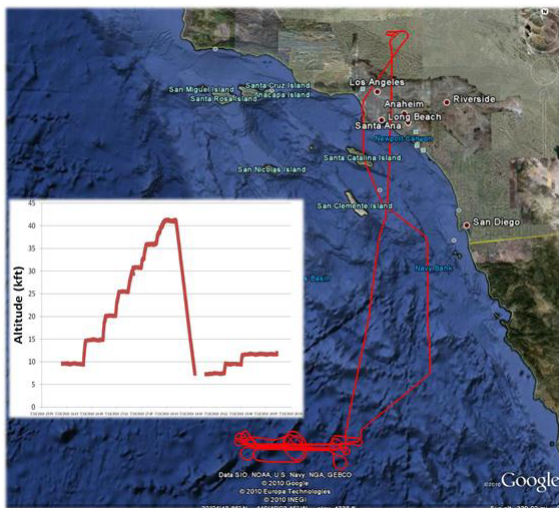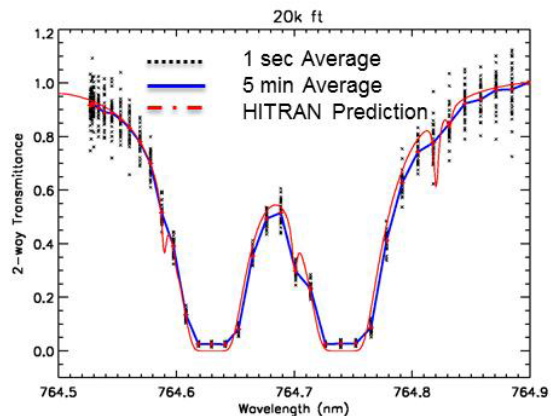

Figure 5 Airborne

Figure 5 Airborne

Figure 7 shows the comparison between the predicted 20 km lineshape (red) and the 1 sec and a 5 min average (blue) at the same altitude. The theory compares favorably with the experimental data but more analysis is needed to implement a true retrieval algorithm for the pressure and correct for instrumental effects like SPCM dead time. We are in the process of implementing these corrections and improvements as well as doing a new airborne campaign in the summer of 2011.

4. SUMMARY

Oxygen measurements are needed for accurate measurements of greenhouse gas mixing ratios (CO2) on a global scale. In order to derive the CO2 concentration in the atmosphere in terms of mole fraction in unit of parts-per-million (ppmv) with regard to dry air, both CO2 and dry air number of molecules in the atmosphere are needed. Since O2 is stable and uniformly mixed in the atmosphere the measurement of O2 absorption in the atmosphere can thus be used to infer dry air number of molecules and then be used to calculate CO2 concentration. We have demonstrated on atmospheric Oxygen measurements using a fiber-based laser system from an airborne platform.

5. REFERENCES

[1] C. L. Korb and C. Y. Wang, Appl. Opt. 22, 3759 (1983).

[2] K. J. Ritter, Ph.D. dissertation submitted to the University of Maryland Graduate School (1986).

[3] G. K. Schwemmer, M. Dombrowski, C. L. Korb, J. Milrod, H. Walden, and R. H. Kagann, Rev. Sci Instrum. 58, 2226 (1987).

[4] C. N. Flamant, G. K. Schwemmer, C. L. Korb, K. D. Evans, and S. P. Palm, J. Atmos. Ocean. Technol. 16, 561 (1999).Author3 X. Y., Z. Author4, 2007: Journal Article Title 2, *Journal Name*, **10**, pp. 25-30, 2007.

[5] Narrowband, tunable, frequency-doubled, erbiumdoped fiber-amplifed transmitter, Mark Stephen, Michael Krainak, Haris Riris, and Graham R. Allan, Opt. Letters, **32**, 2073-2075 (2007)

[6] L. S. Rothman, et. al., "The HITRAN 2008 molecular spectroscopic database," Journal of Quantitative Spectroscopy and Radiative Transfer, 110, (2009).

[7] Abshire, J.B., Riris. H., Allan, G., Weaver C.J., Mao, J. Xiaoli Sun, X., Hasselbrack, W.E., Kawa, R.S, and Biraud, S., "Pulsed airborne lidar measurements of atmospheric CO_2 column absorption", Tellus, 62B, 770–783, (2010)